Table 2. Analysis of the segregation of the AChR subunit genes and other known chromosomal markers in the backcross. Results are shown, in the lower left quadrant of the matrix, as cosegregants per total number of animals analyzed and, in its upper right quadrant, as percentages of cosegregants.

Locus	*Glo-1*	α Actin	α AChR	MHC_F	β AChR	*Idh-1*	MLC_F	γ AChR	δ AChR
Glo-1		47	42	50	50	39	44	44	46
α-Cardiac actin	17/36		81	60	60	51	57	52	54
α-Chain AChR	15/36	34/42		50	50	54	52	48	46
MHC_F	18/36	25/42	21/42		100	57	55	60	61
β-Chain AChR	18/36	25/42	21/42	42/42		57	55	60	61
Idh-1	14/36	19/37	20/37	21/37	21/37		95	89	89
$MLC1_F/MLC3_F$	16/36	24/42	22/42	23/42	23/42	35/37		95	95
γ-Chain AChR	16/36	22/42	20/42	25/42	25/42	33/37	40/42		100
δ-Chain AChR	16/35	22/41	19/41	25/41	25/41	32/36	39/41	41/41	

locus and the γ/δ-subunit genes, the three loci must be arranged in the following order: γ/δ-subunit genes—$MLC1_F/MLC3_F$ genes—*Idh-1*.

Our results are thus consistent with a distribution of the genes coding for the four AChR subunits on three different chromosomes in the mouse. The γ- and δ-subunit genes, which are linked on the same chromosome, are also the most homologous [57% at the amino acid level, compared to 36 to 43% for any other pair of the four genes in *Torpedo marmorata* (*4*)]. Either the γ/δ-subunit gene duplication took place later in evolution compared to the duplication of the α/β subunit, or, as in the case of the immunoglobulin genes, the close proximity of the two genes have maintained their high sequence homology via gene conversion (*14, 15*). However, evidence for this last possibility would require more extensive nucleotide sequence comparisons, in particular between allelic forms of the two genes. The partial dispersion of the four AChR subunit genes suggests that their expression is regulated by *trans*-activating factors rather than by a common *cis* regulatory mechanism. However, it is interesting that the genes for all four subunits of the AChR cosegregate with genes for contractile proteins that are expressed coordinately with them at the onset of myotube formation. Yet, the genetic distances between α-cardiac actin and AChR α-subunit genes (20 cM) and between $MLC1_F/MLC3_F$ and γ/δ-subunit genes (5 cM) correspond to considerable lengths of the DNA molecule that are not likely to form chromatin domains (*16*) responsible for the coordinate activation of these genes during myogenesis.

REFERENCES AND NOTES

1. D. J. Anderson and G. Blobel, *Proc. Natl. Acad. Sci. U.S.A.* **78**, 5598 (1981).
2. J. P. Changeux, A. Devillers-Thiéry, P. Chemouilli, *Science* **225**, 1335 (1984).
3. M. A. Raftery, M. Hunkapiller, C. Strader, L. E. Hood, *ibid.* **208**, 1454 (1980).
4. M. Noda *et al.*, *Nature (London)* **302**, 528 (1983).
5. P. Nef, A. Mauron, R. Stalder, C. Alliod, M. Ballivet, *Proc. Natl. Acad. Sci. U.S.A.* **81**, 7975 (1984).
6. S. Shibahara *et al.*, *Eur. J. Biochem.* **146**, 15 (1985).
7. B. Robert *et al.*, *Nature (London)* **314**, 181 (1985).
8. H. Czosnek *et al.*, *EMBO J.* **2**, 1977 (1983).
9. R. J. LaPolla, K. Mixter Mayne, N. Davidson, *Proc. Natl. Acad. Sci. U.S.A.* **81**, 7970 (1984).
10. A. Klarsfeld, A. Devillers-Thiéry, J. Giraudat, J. P. Changeux, *EMBO J.* **3**, 35 (1984).
11. J.-P. Merlie, R. Sebbane, S. Gardner, E. Olson, J. Lindstrom, *Cold Spring Harbor Symp. Quant. Biol.* **48**, 135 (1983).
12. B. A. Taylor, in *Origins of Inbred Mice*, H. Morse, Ed. (Academic Press, New York, 1978), pp. 423–438.
13. A. Weydert *et al.*, *Proc. Natl. Acad. Sci. U.S.A.* **82**, 7183 (1985).
14. D. Baltimore, *Cell* **24**, 592 (1981).
15. R. Ollo and F. Rougeon, *ibid.* **32**, 515 (1983).
16. N. Hutchison and H. Weintraub, *ibid.* **43**, 471 (1985).
17. E. J. Southern, *J. Mol. Biol.* **98**, 503 (1975).
18. K. E. Isenberg, J. Mudd, V. Shah, J. P. Merlie, *Nucleic Acids Res.* **14**, 5111 (1986).
19. A. Buonanno, J. Mudd, J. P. Merlie, *J. Biol. Chem.*, in press.
20. M. Green, Ed., *Genetic Variants and Strains of the Laboratory Mouse* (Fischer, Stuttgart, 1981).
21. H. Harris and D. A. Hopkinson, *Handbook of Enzyme Electrophoresis in Human Genetics* (North-Holland, Amsterdam, 1978).

22. Supported by grants from the National Institutes of Health, the Muscular Dystrophy Association of America, the Ministère de la Recherche et de la Technologie, the Collège de France, and the Centre National de la Recherche Scientifique. We are grateful to N. Davidson for providing the 6H fragment of the BC3H-1 δ subunit. A.B. was supported by a fellowship from Consejo Nacional de Ciencia y Technologia from Venezuela.

4 June 1986; accepted 30 October 1986

Flow Control Among Microvessels Coordinated by Intercellular Conduction

STEVEN S. SEGAL AND BRIAN R. DULING

Optimal distribution of blood flow requires coordination of vasodilation among resistance vessels. During hyperemia, blood vessels dilate upstream from the initiating stimulus. Spreading vasodilation independent of flow changes has not been previously demonstrated. In the present study, iontophoresis of acetylcholine adjacent to single hamster cheek pouch arterioles in situ (diameter, 20 to 37 micrometers) induced a rapid bidirectional dilation that was not attenuated when blood flow was eliminated with vascular occlusion. This finding indicates that a vasodilatory stimulus is conducted along the arteriole and demonstrates the existence of a mechanism of intercellular communication that is capable of coordinating diameter changes among resistance vessels.

VASODILATION MUST BE COORDINATED among various segments of the peripheral vasculature in order to accurately match blood flow with cellular metabolic demand. Coordination of vasodilation between feed arteries and microvessels is required because there is a substantial pressure drop across the small arteries (100 to 300 μm in diameter) feeding the microcirculation of many tissues (*1*). Thus both feed arteries and arterioles must dilate to achieve the observed increases in blood flow (*1*). An increase in vascular conductance initiated in arterioles intimately associated with the parenchymal cells can induce a complementary dilation of the feed arteries upstream through a flow-dependent mechanism (*2*), apparently mediated by an increase in shear stress acting on the endothelium (*3*).

Within the arteriolar network (vessel diameters less than 60 μm), resistance is also partitioned among and between vessel segments, and a spreading vasodilation has been observed in these vessels (*4, 5*). Whether this spreading dilation is dependent on flow changes or on some other form of conducted response is unknown. Since electrotonic conduction occurs in both isolated endothelial cells and vascular smooth muscle (*6, 7*), we examined the possibility that the coordination of vasodilation within arterioles is due to some form of intercellular communication. We report that acetylcholine (ACh) triggers an arteriolar dilation that is conducted along the vessel wall and is independent of blood flow.

Department of Physiology, University of Virginia School of Medicine, Charlottesville, VA 22908.

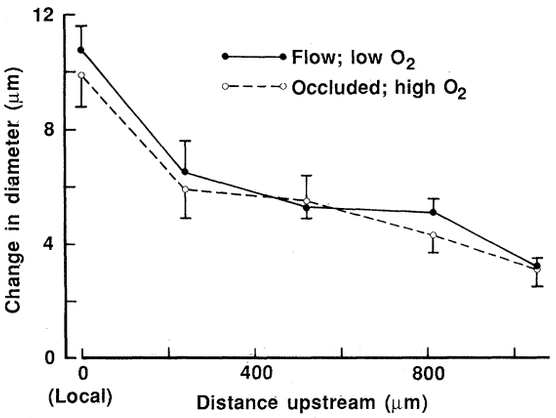

Fig. 1. Summary data (mean ± SEM) for acetylcholine-induced propagated vasodilation in hamster cheek pouch arterioles (n = 12). Eight hamsters were studied during these experiments: in four hamsters, two separate vessels were studied; one vessel was studied in each of the other four animals. Diameter responses during flow and during occlusion were measured at identical locations with each vessel studied. The ordinate values were calculated as the peak internal diameter observed in response to an acetylcholine stimulus minus the resting internal diameter; these values were obtained at the vessel locations indicated on the abscissa. Diameter responses during occlusion were not statistically different from those during flow ($P > 0.3$; paired t tests). Resting internal diameter for these vessels was 29 ± 2 μm (mean ± SEM) during flow and during occlusion.

To test the flow dependence of the spreading dilation in microvessels, we applied ACh by iontophoresis to sites adjacent to single arterioles of the hamster cheek pouch during control (free flow) conditions and again after arteriolar occlusions (*8*). During free flow, after a 1- to 3-second delay, an ACh pulse typically induced a transient local vasodilation that peaked after 7 to 8 seconds and waned by 15 to 20 seconds. The dilation spread rapidly along the arteriole, declining in magnitude with distance from the origin of the stimulus (*9*) (Fig. 1). Iontophoresis of NaCl at the same location was without effect at either local or upstream locations. An identical ACh stimulus applied at 215 to 1075 μm away from an arteriole had no effect on the resting diameter. Thus, simple diffusion of ACh cannot explain the spread of arteriolar dilation (*10*).

To determine whether changes in blood flow mediated the spreading arteriolar dilation, we evaluated the response to ACh at the same sites before and after arteriolar occlusion produced by pressing a glass pipette (diameter, 30 to 35 μm) across an arteriole with a micromanipulator. Occlusion usually caused arteriolar dilation, and, to eliminate the possibility of secondary effects due to the diameter change, we increased the oxygen content of the superfusate to return the diameters of vessels to the preocclusion values (*11*). Branching and collateral flow made it difficult to obtain nonflowing arteriolar segments longer than 1000 to 1200 μm. In the occluded vessels, dilation spread along the arteriole with a latency, magnitude, and decay not significantly different from those observed during flow (Fig. 1). The velocity of the response in the absence of flow suggested that the vasodilatory stimulus was propagated along the vessel wall.

Because of the increase in vessel volume during dilation, there was a small influx of blood into the occluded segment. To ascertain that this blood movement was not the proximate stimulus for dilation, we performed four additional experiments using a double occlusion technique in which a segment of an arteriole up to 516 μm long was sealed at both ends with occlusion pipettes to prevent changes in segment volume during applications of ACh (Fig. 2). Acetylcholine was applied distal to the occlusion, and dimensional measurements were made at the site of the ACh pipette, in the occluded segment, and 800 to 1200 μm proximal to the ACh pipette (Fig. 2). As expected, ACh pulses produced no red cell motion and had minimal effect on diameter of the vessel segment located between the occlusion pipettes. In spite of this absence of cell motion, the magnitude of propagated vasodilation during the double occlusions was not different from that observed during flow (*12*) (Fig. 2). These experiments substantiated our finding that a propagated vasodilatory stimulus capable of coordinating vasodilation in contiguous arteriolar segments is not dependent on the motion of blood for its action.

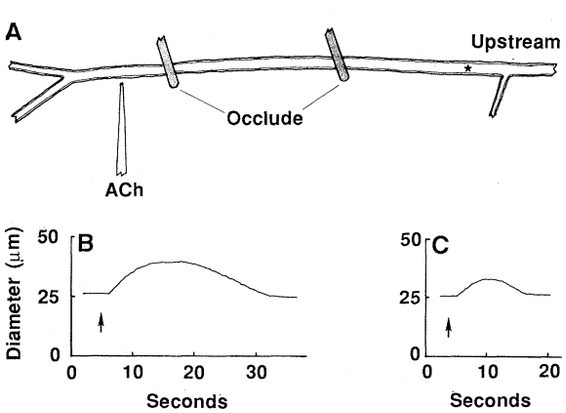

Fig. 2. Conducted vasodilation in a hamster cheek pouch arteriole. The experimental approach is shown by the illustration (A), which was traced from a photograph. Two occlusion pipettes were placed across the arteriole to seal a vessel segment (length, 500 μm); volume changes and fluid motion in the sealed segment were thereby excluded. Acetylcholine (ACh) given at time indicated by the arrow induced dilation locally (B), and a propagated dilation at 1 mm upstream from the ACh pipette (star) (C). This propagated response in the absence of blood flow demonstrates that a dilatory stimulus was conducted along the arteriole. Both local and propagated dilations during flow were similar to those recorded during occlusion.

We attempted to measure propagation velocity by a video technique (*13*) but found that the delay to the onset of dilation was so long relative to the propagation delay that no useful data could be obtained. We estimate that the limit of temporal resolution for propagation velocity by video analysis was approximately 2 mm/sec (*14*). Since there was no measurable difference for the onset of dilation between locations separated by more than 1 mm, we conclude that propagation velocity was in excess of 2 mm/sec and was masked by the delay in response of the smooth muscle to the dilatory stimulus. Further experiments, perhaps with the use of intracellular recording techniques, are required to obtain definitive measures of propagation velocity.

The demonstration of a propagated vasodilation indicates that some form of direct communication between the cells constituting the arteriolar wall coordinates the elements of microvascular resistance. A compelling question is how these cells actually communicate with one another. One obvious pathway by which a vasodilatory stimulus may be conducted along the arteriole involves nerve fibers intrinsic to the vessel wall (*15*). The specificity of the response to ACh (*4, 16*) suggests that a muscarinic pathway may underly the propagation of a vasodilatory stimulus, but it remains to be defined. In conduit arteries, the vasodilatory response to ACh is mediated by endothelial cells (*17*). However, similar studies have yet to be successfully completed in arterioles.

The second obvious pathway for conducting information along the arteriole is via gap junctions, which provide direct electrical and metabolic communication between adjacent cells (*6, 18*). Gap junctions have been shown by ultrastructural techniques to connect smooth muscle cells, endothelial cells, and the endothelium with smooth muscle (*19*). Thus, the arteriole exemplifies a preparation in which intercellular relationships

can be studied in vivo, but there have been too few studies of the physiological interactions between endothelial and smooth muscle cells in the intact arteriole to permit conclusions regarding the role of gap junctions in propagated vasodilation.

REFERENCES AND NOTES

1. D. D. Stromberg and J. R. Fox, *Circ. Res.* **31**, 229 (1972); H. G. Bohlen, R. W. Gore, P. M. Hutchins, *Microvasc. Res.* **13**, 125 (1977); H. G. Bohlen and R. W. Gore, *ibid.* **14**, 251 (1977); S. H. Nellis, A. J. Liedtke, L. Whitesell, *Circ. Res.* **49**, 342 (1981); S. S. Segal and B. R. Duling, *ibid.* **59**, 283 (1986).
2. R. Ingebrigtsen and S. Leraand, *Acta Physiol. Scand.* **79**, 552 (1970); M. Lie, O. M. Sejersted, F. Kiil, *Circ. Res.* **27**, 727 (1970).
3. J. Holtz *et al.*, *Z. Kardiol.* **72**, 98 (1983).
4. B. R. Duling and R. M. Berne, *Circ. Res.* **26**, 163
5. A. Krogh, G. A. Harrop, P. B. Rehberg, *J. Physiol. (London)* **56**, 179 (1922); B. R. Lutz, G. P. Fulton, R. P. Akers, *Exp. Med. Surg.* **8**, 258 (1950); S. S. Segal and B. R. Duling, present observations.
6. D. M. Larson, E. Y. Kam, J. D. Sheridan, *J. Membrane Biol.* **74**, 103 (1983).
7. F. Mekata, *J. Physiol. (London)* **242**, 143 (1974). S. M. Hilton proposed that a vasodilatory stimulus could be conducted along the blood vessel wall [*ibid.* **149**, 93 (1959)].
8. Male hamsters (120 g) were anesthetized with sodium pentobarbital; cheek pouches were prepared for observation of microvessels [B. R. Duling, *Microvasc. Res.* **5**, 423 (1973)]. Esophageal and cheek pouch temperatures were maintained at 37°C. Cheek pouch preparations were superfused continually with a bicarbonate-buffered physiological salt solution (*p*H 7.4) equilibrated with 5% CO_2 and 95% N_2 during free-flow conditions. Glass micropipettes, beveled to an internal tip diameter of 2 μm, were filled with 1.0*M* acetylcholine chloride (Sigma) dissolved in distilled water. The micropipette tip was positioned 4 to 6 μm from the arteriolar wall, and ACh was applied via an iontophoresis programmer (World Precision Instruments, model 160). The retaining current, typically 100 nA, was established as the minimum required to prevent local dilation due to ACh leakage from the pipette tip. Ejection currents were typically 200 msec in duration and 1000 nA in amplitude. Sodium chloride (1.0*M*) was prepared and iontophoresed in a similar fashion as a control. Microvessels were observed by videomicroscopy with transmitted light at a magnification of ×1200. Vessel diameters were recorded continuously with a video analyzer (Colorado 321), the output of which was directed to a chart recorder. To eliminate the potential for convective transport of ACh in arteriolar blood, we observed sites upstream from the point of ACh application. Countercurrent transport of ACh was circumvented either by simultaneous occlusion of adjacent venules or by observing arteriole segments devoid of adjacent venules.
9. The dilation induced by acetylcholine propagates upstream into larger arterioles (diameter, 40 to 60 μm). We have observed propagated vasodilation more than 3700 μm upstream from the stimulus origin.
10. According to the relation $t = \Delta x^2/2D$, where t is time, x is distance, and D is the diffusion coefficient [M. Jacobs, *Ergeb. Biol.* **12**, 1 (1935)], for $D = 10^{-5}$ cm^2/sec (approximate diffusion coefficient for small monovalent cations), diffusion of ACh or a chemical intermediate would require 5 seconds to move 100 μm and 500 seconds to move 1000 μm.
11. The response of arterioles to a vasoactive stimulus varies substantially as a function of vasomotor state. [R. W. Gore, *Am. J. Physiol.* **222**, 82 (1972)]. In control experiments performed during flow, we have observed that the vasoconstriction occurring in response to elevated oxygen did not qualitatively affect propagated vasodilation.
12. At 1029 ± 44 μm (mean ± SEM; $n = 4$) upstream from the ACh pipette, the amplitude of the propagated vasodilation both during flow and during double occlusion was 5.5 ± 0.9 μm; the length of occluded segments was 424 ± 56 μm.
13. For these experiments, a light-emitting diode (LED) was connected in series with the output of the iontophoresis unit and placed at the edge of the optical path to the video camera. In this configuration, the LED flash coincided with the iontophoretic stimulus. Video recordings were obtained of vascular responses adjacent to the micropipette and at measured increments along a vessel. Each video record contained the LED flash and a video timer signal accurate to hundredths of a second. Subsequently, the video record was played back frame by frame, and the interval between the LED flash and the onset of dilation was obtained. Propagation velocity was calculated by subtracting the interval determined at the pipette tip from similar intervals obtained at upstream locations.
14. With video analysis, we estimate that we could discern any delay exceeding 500 msec for the onset of dilation between two locations separated by a distance of 1 mm.
15. There is extensive documentation for both adrenergic and cholinergic arteriolar innervation: B. R. Lutz, G. P. Fulton, R. P. Akers, *Exp. Med. Surg.* **8**, 258 (1950); E. A. Schenk and A. E. Badawi, *Z. Zellforschung* **91**, 170 (1968); G. R. Siggins and H. A. Weitsen, *Microvasc. Res.* **3**, 308 (1971); W. L. Joyner, G. T. Campbell, C. Peterson, J. Wagoner, *ibid.* **26**, 27 (1983). Postganglionic neurons intrinsic to the arteriolar wall have been proposed to mediate vasodilation [H. A. Myers, E. A. Schenk, C. R. Honig, *Am. J. Physiol.* **229**, 126 (1975); C. R. Honig and J. L. Frierson, *ibid.* **230**, 493 (1976)]. In preliminary experiments, we have observed that 10^{-6}*M* tetrodotoxin did not affect the ACh-induced propagated vasodilation.
16. S. S. Segal and B. R. Duling, unpublished observations. Over 90% of the vessels examined demonstrated propagated vasodilation in response to an ACh stimulus. Both local and propagated vasodilation are blocked with 10^{-6}*M* atropine in the superfusate.
17. R. F. Furchgott and J. V. Zawadzki, *Nature (London)* **288**, 373 (1980).
18. N. B. Gilula, O. R. Reeves, A. Steinbach, *ibid.* **235**, 262 (1972); J. D. Pitts and J. W. Simms, *Exp. Cell Res.* **104**, 153 (1977); D. C. Spray, R. L. White, F. Mazet, M. V. L. Bennett, *Am. J. Physiol.* **248**, H753 (1985).
19. J. A. G. Rhodin, *J. Ultrastruct. Res.* **18**, 181 (1967); M. Simionescu, N. Simionescu, G. E. Palade, *J. Cell Biol.* **67**, 863 (1975); R. Taugner, H. Kirchheim, W. G. Forssmann, *Cell Tissue Res.* **235**, 319 (1984).

20. A preliminary report of these data was presented at the 1986 FASEB meetings. We thank D. N. Damon for his technical assistance and C. Desjardins for his critique of this manuscript. Supported by the NIH grants HL06947 and HL12792.

11 June 1986; accepted 23 September 1986

Vertical Nitrate Fluxes in the Oligotrophic Ocean

MARLON R. LEWIS, W. GLEN HARRISON, NEIL S. OAKEY, DAVID HEBERT, TREVOR PLATT

The vertical flux of nitrate across the thermocline in the upper ocean imposes a rigorous constraint on the rate of export of organic carbon from the surface layer of the sea. This export is the primary means by which the oceans can serve as a sink for atmospheric carbon dioxide. For the oligotrophic open ocean regions, which make up more than 75% of the world's ocean, the rate of export is currently uncertain by an order of magnitude. For most of the year, the vertical flux of nitrate is that due to vertical turbulent transport of deep water rich in nitrate into the relatively impoverished surface layer. Direct measurements of rates of turbulent kinetic energy dissipation, coupled with highly resolved vertical profiles of nitrate and density in the oligotrophic eastern Atlantic showed that the rate of transport, averaged over 2 weeks, was 0.14 (0.002 to 0.89, 95% confidence interval) millimole of nitrate per square meter per day and was statistically no different from the integrated rate of nitrate uptake as measured by incorporation of ^{15}N-labeled nitrate. The stoichiometrically equivalent loss of carbon from the upper ocean, which is the relevant quantity for the carbon dioxide and climate question, is then fixed at 0.90 (0.01 to 5.70) millimole of carbon per square meter per day. These rates are much lower than recent estimates based on in situ changes in oxygen over annual scales; they are consistent with a biologically unproductive oligotrophic ocean.

IN CONTEMPORARY, GLOBAL, GEOchemical models of the atmosphere-ocean carbon cycle, the oceans are viewed as the primary sink for atmospheric carbon dioxide (*1*). The responsible mechanism is the photosynthetic incorporation of dissolved carbon dioxide by marine microalgae in the upper ocean, followed by vertical loss of organic carbon, either through sinking particles or associated with vertical fluid transport. For the open ocean regions, which make up more than 75% of the world's oceans, both the rate of photosynthetic incorporation (the so-called total production) and the rate of export of organic carbon ("new" production) are currently uncertain to within an order of magnitude (*2*). Given the profound importance of the oceans in the global carbon cycle, this uncertainty propagates to a much greater uncertainty in prediction of future atmospheric carbon dioxide concentrations and hence in

M. R. Lewis and D. Hebert, Department of Oceanography, Dalhousie University, Halifax, Nova Scotia, B3H 4J1 Canada.
W. G. Harrison and T. Platt, Department of Fisheries and Oceans, Marine Ecology Laboratory, Bedford Institute of Oceanography, Dartmouth, Nova Scotia, B2Y 4A2 Canada.
N. S. Oakey, Department of Fisheries and Oceans, Atlantic Oceanographic Laboratory, Bedford Institute of Oceanography, Dartmouth, Nova Scotia, B2Y 4A2 Canada.